

SUPPORTING INFORMATION

Supported C₆₀-IL-PdNP as extremely active nanocatalysts for C–C cross coupling reactions

Francesco Giacalone,^a Vincenzo Campisciano,^a Carla Calabrese,^{a,b} Valeria La Parola,^c*

*Leonarda F. Liotta,^c Carmela Aprile,^b Michelangelo Gruttaduria^a**

^a Dipartimento Scienze e Tecnologie Biologiche, Chimiche e Farmaceutiche (STEBICEF), Università degli Studi di Palermo, Viale delle Scienze, Ed. 17, 90128 Palermo (Italy).
Email: francesco.giacalone@unipa.it, Tel: +39 09123897530.
michelangelo.gruttaduria@unipa.it. Tel: +39 09123897534.

^b Laboratory of Applied Material Chemistry (CMA), University of Namur, 61 rue de Bruxelles, 5000 Namur (Belgium).

^c Istituto per lo Studio dei Materiali Nanostrutturati ISMN-CNR, Via Ugo La Malfa 153, 90146- Palermo (Italy).

Table of Contents

Figure S1. N₂-adsorption/desorption isotherms and pore size distribution of amorphous silica and **4a**.

Figure S2. N₂-adsorption/desorption isotherms and pore size distribution of SBA-15 and **4b**.

Figure S3. Experimental X-ray diffraction pattern of materials **5a-c** and simulated diffraction pattern of palladium and maghemite.

Figure S4. HR-TEM of **5a**.

Table S1. XPS Pd 3d_{5/2} binding energies (eV), Pd/Si, Pd/C, N/Si and N/C surface atomic ratios.

Figure S5. Solid-state ¹³C NMR of materials **4a** and **5a**.

Table S2. Screening of reaction conditions and dependence of reaction yield in function of the temperature in the reaction between 4-iodoanisole and methylacrylate.

Figure S6. Recycling tests of catalysts **5b** and **5c** in the Suzuki reaction.

Figure S7. High-resolution XPS of Pd3d region of fresh and reused **5a**.

List of ¹H NMR spectral data of pure known compounds S7 – S8

¹H NMR spectra of pure known compounds and those of partially converted mixtures of Heck and Suzuki reactions S9 – S19

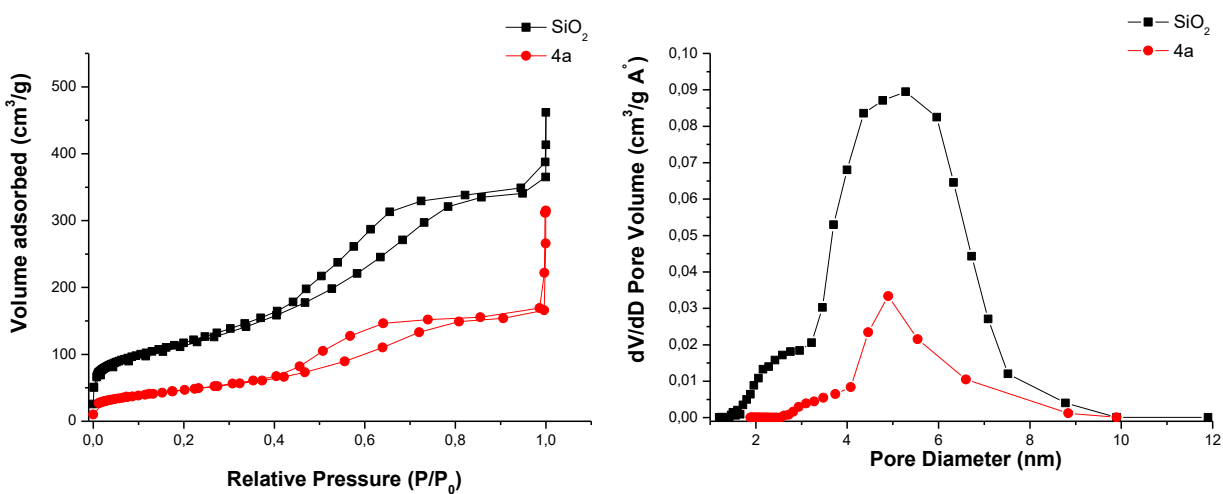


Figure S1. N₂-adsorption/desorption isotherms and pore size distribution of amorphous silica and **4a**.

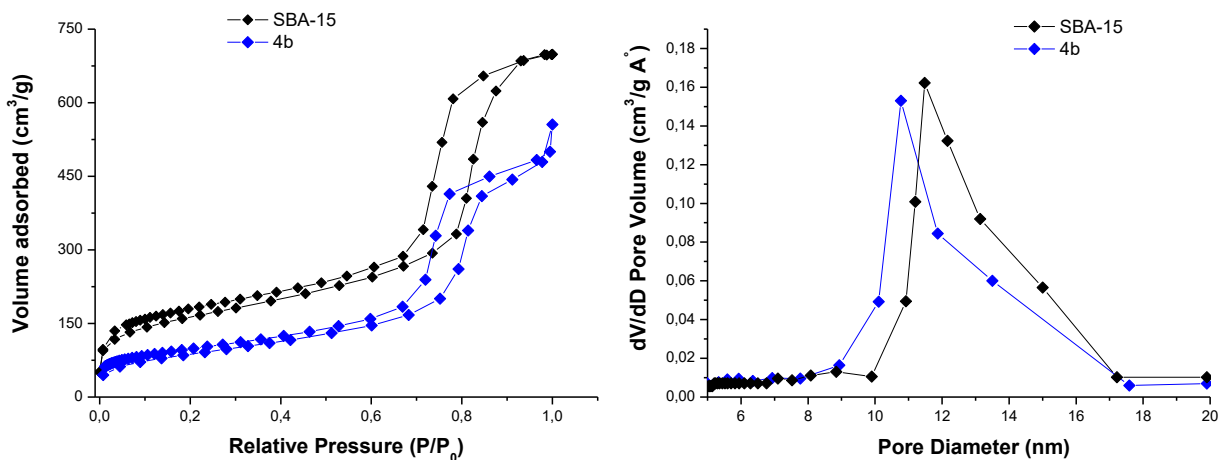


Figure S2. N₂-adsorption/desorption isotherms and pore size distribution of SBA-15 and **4b**.

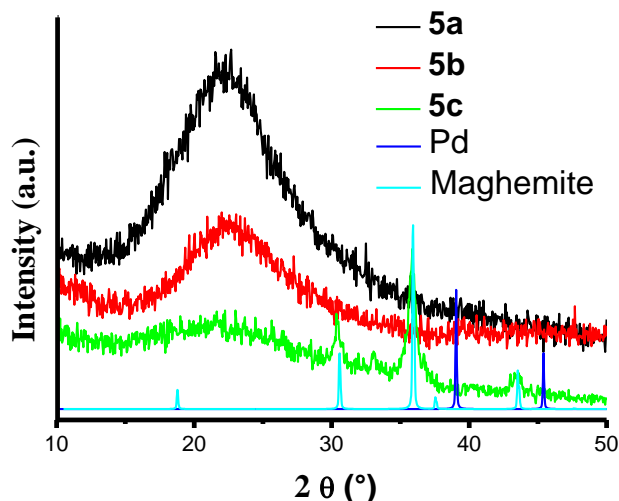


Figure S3. Experimental X-ray diffraction pattern of materials **5a-c** and simulated diffraction pattern of palladium and maghemite.

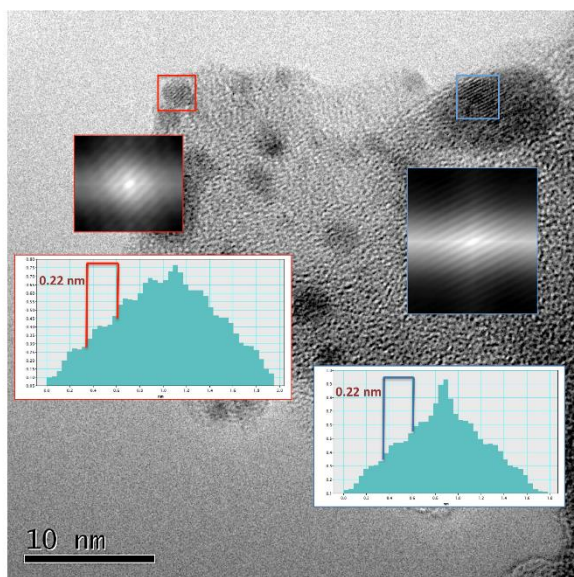


Figure S4. HR-TEM of **5a**. Fast Fourier transform (FFT) patterns and autocorrelation profiles are reported in the red and blue squares.

Table S1. XPS Pd 3d_{5/2} binding energies (eV), Pd/Si, Pd/C, N/Si and N/C surface atomic ratios. The relative percentages are given in parentheses.

Material	Pd 3d _{5/2}	Pd/Si	Pd/C	N/Si	N/C
5a	334.9 (42)				
	336.9 (58)	0.025	0.010	0.11	0.04
5b	334.9 (46)				
	337 (54)	0.024	0.008	0.08	0.03
5c	335.3 (37)				
	337.6(63)	0.094	0.005	0.52	0.03

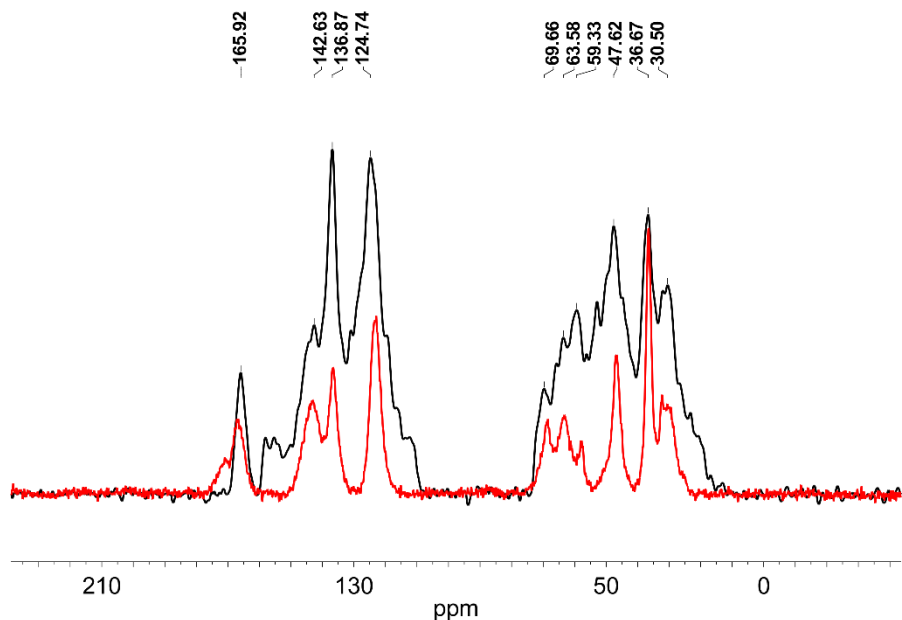
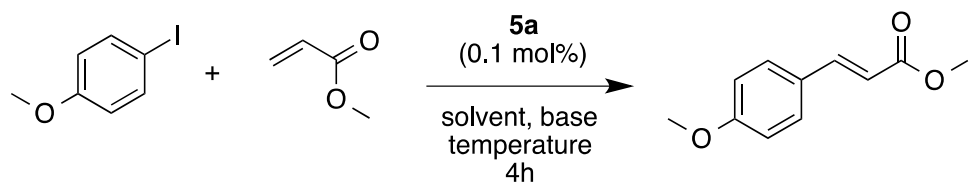


Figure S5. Solid-state ^{13}C NMR of materials **4a** (red) and **5a** (black).

Table S2. Screening of reaction conditions and dependence of reaction yield in function of the temperature in the reaction between 4-iodoanisole and methylacrylate.



Entry	Solvent	Base	Temperature / $^{\circ}\text{C}$	Yield ^b %
1	Toluene	NEt_3	100	22
2	Acetonitrile	NEt_3	100	82
3	$\text{H}_2\text{O}/\text{EtOH}$ (1:3)	K_2CO_3	100	31
4	DMF	NEt_3	120	>99
5	DMF	NEt_3	90	85
6	DMF	NEt_3	60	0

^a Reaction conditions: methyl acrylate (0.75 mmol), 4-iodoanisole (0.5 mmol), base (1 mmol), solvent (1 mL), catalyst (0.1 mol%, 2.5 mg). ^b After purification.

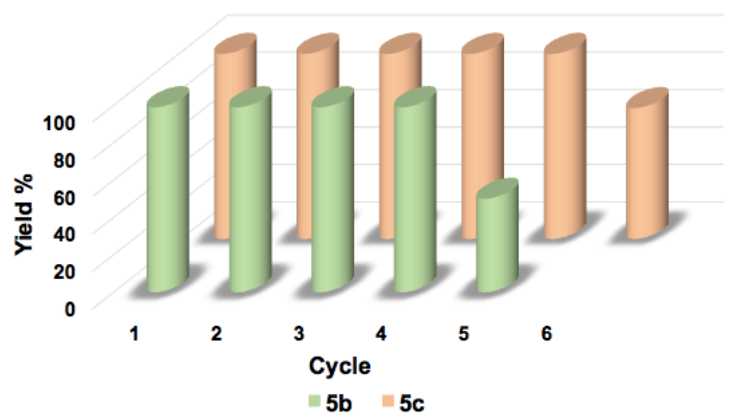
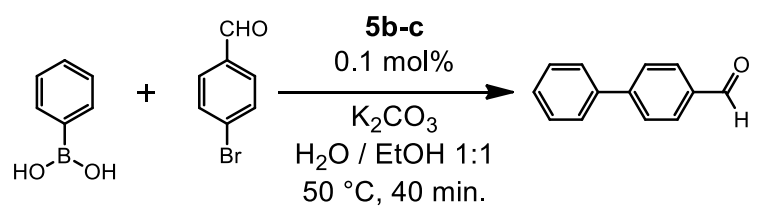


Figure S6. Recycling tests of catalysts **5b** and **5c** in the Suzuki reaction.

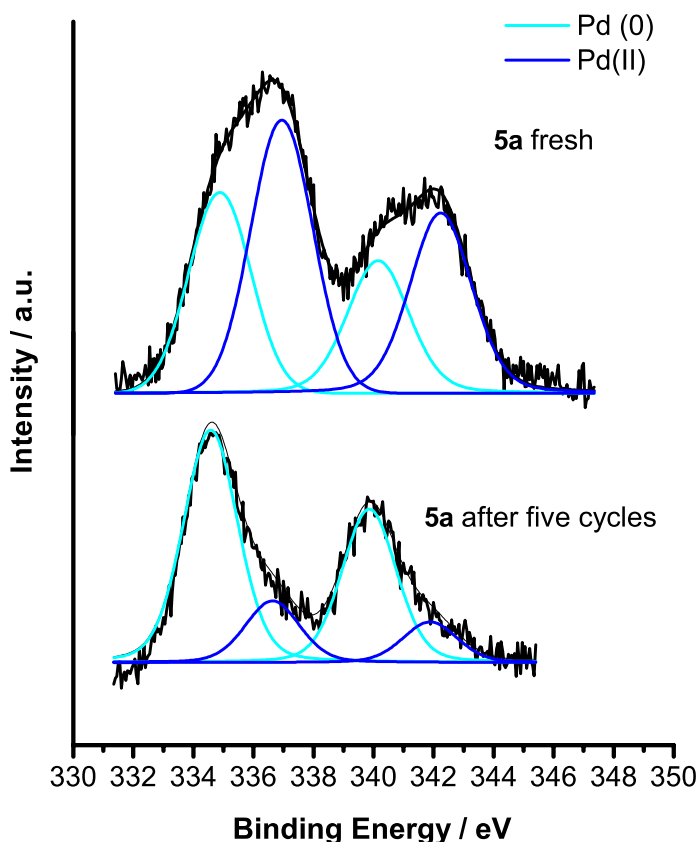
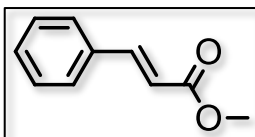
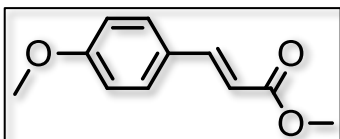


Figure S7. High-resolution XPS of Pd3d region of fresh **5a** (up) and reused **5a** for five times (bottom).

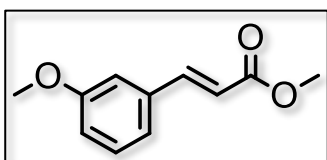
List of ^1H NMR spectral data of pure known compounds:



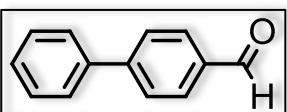
(E)-Methyl Cinnamate; ^1H NMR (CDCl_3 , 300 MHz): δ 7.71 (d, 1H, $J = 16.0$ Hz), 7.55–7.52 (m, 2H), 7.40–7.38 (m, 3H), 6.45 (d, 1H, $J = 16.0$ Hz), 3.82 (s, 3H).



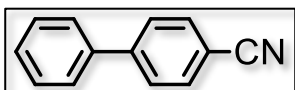
(E)-Methyl-4-methoxycinnamate; ^1H NMR (CDCl_3 , 300 MHz): δ 7.66 (d, 1H, $J = 16.0$ Hz), 7.49 (d, 2H, $J = 8.7$ Hz), 6.91 (d, 2H, $J = 8.7$ Hz), 6.32 (d, 1H, $J = 16.0$ Hz), 3.85 (s, 3H), 3.80 (s, 3H).



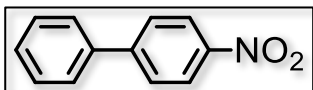
(E)-Methyl 3-methoxycinnamate; ^1H NMR (CDCl_3 , 300 MHz): δ 7.66 (d, 1H, $J = 16.0$ Hz), 7.32–7.27 (m, 1H), 7.12–7.10 (m, 1H), 7.03–7.04 (m, 1H), 6.95–6.92 (m, 1H), 6.43 (d, 1H, $J = 16.0$ Hz), 3.82 (s, 3H) 3.80 (s, 3H).



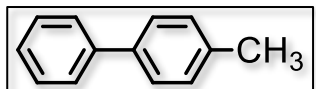
4-Formylbiphenyl; ^1H NMR (300 MHz, CDCl_3 , ppm): δ 10.08 (s, 1H), 7.97 (d, 2H, $J = 7.7$ Hz), 7.77 (d, 2H, $J = 7.7$ Hz), 7.66 (d, 2H, $J = 7.5$ Hz), 7.52–7.43 (m, 3H).



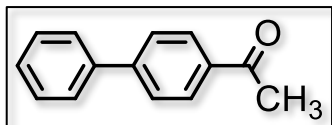
4-Cyanobiphenyl; ^1H NMR (300 MHz, CDCl_3 , ppm): δ 7.76–7.68 (m, 4H), 7.62–7.59 (m, 2H), 7.51–7.42 (m, 3H).



4-Nitrobiphenyl; ^1H NMR (300 MHz, CDCl_3 , ppm): δ 8.32 (d, 2H, $J = 8.7$ Hz), 7.76 (d, 2H, $J = 8.7$ Hz), 7.64 (d, 2H, $J = 6.7$ Hz), 7.54–7.46 (m, 3H).



4-Methylbiphenyl; **¹H NMR** (300 MHz, CDCl₃, ppm): δ 7.60 (d, 2H, *J* = 7.3 Hz), 7.54–7.42 (m, 4H), 7.37–7.34 (m, 1H), 7.28 (d, 2H, *J* = 7.9 Hz), 2.42 (s, 3H).



4-Acetyl biphenyl; **¹H NMR** (300 MHz, CDCl₃, ppm): δ 8.05 (d, 2H, *J* = 8.4 Hz), 7.71–7.63 (m, 4H), 7.51–7.40 (m, 3H), 2.65 (s, 3H).

¹H NMR spectra of pure known compounds and those of partially converted mixtures of Heck and Suzuki reactions:

